Engineering Notes

ENGINEERING NOTES are short manuscripts describing new developments or important results of a preliminary nature. These Notes should not exceed 2500 words (where a figure or table counts as 200 words). Following informal review by the Editors, they may be published within a few months of the date of receipt. Style requirements are the same as for regular contributions (see inside back cover).

Rigid Body Rate Inference from Attitude Variation

Itzhack Y. Bar-Itzhack*
Technion—Israel Institute of Technology, 32000 Haifa, Israel
Richard R. Harman†
NASA Goddard Space Flight Center, Greenbelt, Maryland 20771
and
Julie K. Thienel‡
U.S. Naval Academy, Annapolis, Maryland 21402

DOI: 10.2514/1.23955

I. Introduction

THIS Note deals with the extraction of the angular velocity in a gyroless spacecraft (SC) for which the attitude is represented by a quaternion that is obtained as a measurement of autonomous star trackers (AST) [1]. When the attitude is known, one can differentiate it and use the kinematics equation that connects the derivative of the attitude with the satellite angular rate to compute the latter [2,3]. However, because the attitude is obtained from sensor measurements, it introduces considerable noise. Another approach employs a Kalman filter (KF) using the SC rotational kinematics equation [4,5]. However, the use of a KF requires the computation of a covariance matrix. Not only is this process cumbersome, sometimes it may also pose an accuracy problem. This accuracy problem led to the use of the more computationally intensive covariance measurement-update formula [6], square root filtering [7], and other sophisticated approaches.

In this work, we investigate simple algorithms that do not require a covariance computation. In particular, we investigate the use of passive feedback loops for extracting the angular velocity from the measured attitude quaternion for control loop damping. In our approach, the dominant factor is simplicity rather than accuracy, because normally, crude rate information is often sufficient for damping. We start our investigation in the next section with an examination of the pseudolinear Kalman (PSELIKA) filter [8]. In particular, we consider the filter gain when the filter tracks the SC rates well. Some particular characteristics of the gain are observed and analytically proven. All the algorithms are tested with quaternion inputs. The tests prove that the algorithms are suitable for rate-estimation extraction for control loop damping.

Received 16 March 2006; revision received 8 September 2006; accepted for publication 9 September 2006.

*Professor Emeritus, Faculty of Aerospace Engineering; ibaritz@tx.technion.ac.il. Member Technion Asher Space Research Institute. Fellow IEEE. Fellow AIAA.

†Aerospace Engineer, Flight Dynamics Analysis Branch, Code 595; richard.r.harman@nasa.gov.

‡Assistant Professor, Department of Aerospace Engineering; thienel@usna.edu.

II. Angular Rate Determination by Estimation

The rate of change of the quaternion is described by the well-known equation (e.g., see [9], p. 512):

$$\dot{\boldsymbol{q}} = \tfrac{1}{2} Q \boldsymbol{\omega} \tag{1a}$$

$$Q = \begin{bmatrix} qI_3 + [\boldsymbol{e}\times] \\ -\boldsymbol{e}^T \end{bmatrix} \tag{1b}$$

where $\boldsymbol{\omega}$ is the angular velocity vector; the elements q and $\boldsymbol{e}$ are, respectively, the scalar part and the vector part of the quaternion, that is, $\boldsymbol{q}^T = [\,\boldsymbol{e}^T \quad q\,]$; I_n is the n-dimensional identity matrix; and $[\boldsymbol{e}\times]$ is the cross-product matrix of the vector $\boldsymbol{e}$, which is given by

$$[\boldsymbol{e}\times] = \begin{bmatrix} 0 & -e_z & e_y \\ e_z & 0 & -e_x \\ -e_y & e_x & 0 \end{bmatrix} \tag{1c}$$

where e_x, e_y, and e_z are the components of $\boldsymbol{e}$.

The angular dynamics of a rigid body SC is given in the following equation ([9], p. 523):

$$\dot{\boldsymbol{\omega}} = J^{-1}[(J\boldsymbol{\omega} + \boldsymbol{h})\times]\boldsymbol{\omega} + J^{-1}(\boldsymbol{T} - \dot{\boldsymbol{h}}) \tag{2}$$

where J is the SC inertia matrix, $\boldsymbol{h}$ is the angular momentum of the momentum wheels, and $\boldsymbol{T}$ is the external torque acting on the SC. We can augment Eqs. (1a) and (2) and, for filter stability purposes, add white-noise vectors [10]. This yields the state space augmented equation:

$$\begin{bmatrix} \dot{\boldsymbol{q}} \\ \dot{\boldsymbol{\omega}} \end{bmatrix} = \begin{bmatrix} 0_{4\times4} & \tfrac{1}{2}Q \\ 0_{3\times4} & J^{-1}[(J\boldsymbol{\omega} + \boldsymbol{h})\times] \end{bmatrix} \begin{bmatrix} \boldsymbol{q} \\ \boldsymbol{\omega} \end{bmatrix} + \begin{bmatrix} \boldsymbol{0} \\ J^{-1}(\boldsymbol{T} - \dot{\boldsymbol{h}}) \end{bmatrix} + \begin{bmatrix} \boldsymbol{w}_q \\ \boldsymbol{w}_\omega \end{bmatrix} \tag{3a}$$

In the case considered, in which the measured entity is the quaternion itself, the measurement model is

$$\boldsymbol{q}_m = [\, I_4 \quad 0_{4\times3} \,] \begin{bmatrix} \boldsymbol{q} \\ \boldsymbol{\omega} \end{bmatrix} + \boldsymbol{v}_q \tag{3b}$$

where $\boldsymbol{q}_m$ is the measurement, and $\boldsymbol{v}_q$ is an appropriate measurement noise. Equations (3) have been used to estimate the angular rate with much success, either after linearization, using an extended Kalman filter (EKF) [11,12] or after a simple manipulation, using a PSELIKA filter [8]. In fact, when the measurements come at a relatively fast rate, satisfactory rate estimates can be achieved when the nonlinear SC dynamics model of Eq. (2) is replaced by the following simple linear Markov model [4]:

$$\dot{\boldsymbol{\omega}} = -N\boldsymbol{\omega} + \boldsymbol{w}_\omega \tag{4a}$$

$$N = -nI_3 \tag{4b}$$

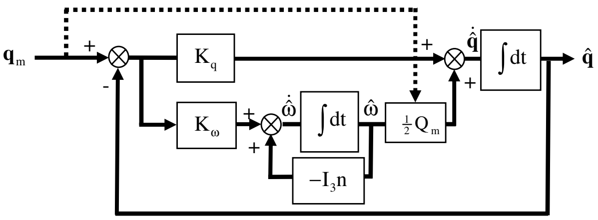

Fig. 1 Block diagram representation of the PSELIKA filter rate estimator.

where n is an inverted time constant, and $\boldsymbol{w}_\omega$ is an appropriate noise vector.[§] In this case, we obtain the following model:

$$\begin{bmatrix} \dot{\boldsymbol{q}} \\ \dot{\boldsymbol{\omega}} \end{bmatrix} = \begin{bmatrix} 0_{4\times 4} & \frac{1}{2}Q \\ 0_{3\times 4} & -nI_3 \end{bmatrix} \begin{bmatrix} \boldsymbol{q} \\ \boldsymbol{\omega} \end{bmatrix} + \begin{bmatrix} \boldsymbol{w}_q \\ \boldsymbol{w}_\omega \end{bmatrix} \tag{5}$$

As seen in the following continuous general linear KF algorithm,

$$\dot{\hat{\boldsymbol{x}}} = F\hat{\boldsymbol{x}} + K[z - H\hat{\boldsymbol{x}}] \tag{6}$$

a KF of any kind (or a Luenberger observer [13]) operates as a feedback system. In our case, Eq. (6) becomes

$$\begin{bmatrix} \dot{\hat{\boldsymbol{q}}} \\ \dot{\hat{\boldsymbol{\omega}}} \end{bmatrix} = \begin{bmatrix} -K_q & \frac{1}{2}Q \\ -K_\omega & -nI_3 \end{bmatrix} \begin{bmatrix} \hat{\boldsymbol{q}} \\ \hat{\boldsymbol{\omega}} \end{bmatrix} + \begin{bmatrix} K_q \\ K_\omega \end{bmatrix} \boldsymbol{q}_m \tag{7}$$

A block diagram realization of the last equation is shown in Fig. 1. Note that Q is a function of $\hat{\boldsymbol{q}}$. In fact, because the AST yields very accurate quaternions, we can initially use $\boldsymbol{q}_m$ rather than $\hat{\boldsymbol{q}}$ to evaluate Q. The Kalman gain components K_q and K_ω are, of course, computed as a part of the usual gain computation of the KF.

Although in practice, the discrete formulation of the filter algorithms is implemented, we interchangeably use the continuous formulation to investigate certain qualities of the filters. This is permissible because the effect of a continuous filter can be considered as that of a discrete filter running at an extremely small step size between measurements.

A. Qualities of K_q and K_ω

In estimating the angular velocity using quaternion measurements and the PSELIKA filter, the gains K_q and K_ω have special forms that could be used to our computational advantage. To explore these qualities, it is convenient to consider the continuous KF algorithm as a discrete algorithm. Omitting, for convenience, time labeling, the formula for computing the discrete Kalman gain is

$$K = P(-)H^T[HP(-)H^T + R]^{-1} \tag{8}$$

where $P(-)$ is the a priori covariance matrix, H is the measurement matrix, and R is the covariance matrix of the measurement noise, all at time t_k. From Eq. (3b)

$$H = \begin{bmatrix} I_4 & 0_{4\times 3} \end{bmatrix} \tag{9}$$

For this particular measurement matrix, one obtains

$$K = \begin{bmatrix} P_{11}(-)[P_{11}(-) + R]^{-1} \\ P_{12}^T(-)[P_{11}(-) + R]^{-1} \end{bmatrix} \tag{10a}$$

where $P_{11}(-)$ and $P_{12}(-)$ are submatrices of $P(-)$, as seen here:

$$P(-) = \begin{bmatrix} P_{11}(-) & P_{12}(-) \\ P_{12}^T(-) & P_{22}(-) \end{bmatrix} \tag{10b}$$

From Eq. (10a), we obtain

$$K_q = P_{11}(-)[P_{11}(-) + R]^{-1} \tag{10c}$$

[§]It should be noted that this is just a model and not the true description of the rate vector dynamics.

$$K_\omega = P_{12}^T(-)[P_{11}(-) + R]^{-1} \tag{10d}$$

We present the special features of K_q and K_ω in the following proposition.

Proposition: Let $P_0 = \mathrm{diag}\{\, p_{q,0}I_4 \quad p_{\omega,0}I_3 \,\}$, $G = \mathrm{diag}\{\, \eta_q I_4 \quad \eta_\omega I_3 \}$, and $R = \xi I_4$, where P_0 is the initial covariance matrix, G is the state driving-noise covariance matrix, and R is the measurement noise covariance matrix, all as used in the covariance computation channel[¶]; then, to first order, K_q is a diagonal matrix and K_ω takes the form $\upsilon[\, pI_3 + [-\boldsymbol{r}\times] \mid \; -\boldsymbol{r}\,]$, where υ and p are scalars and $\boldsymbol{r}$ is a 3-D vector. In fact, K_ω is of the form $\upsilon Q(\boldsymbol{q})^T$, where $\boldsymbol{q}$ is some attitude quaternion.

Proof: Consider the transition matrix from time t_{k-1} to t_k. Let $\Delta = t_k - t_{k-1}$, then the transition matrix A is given by $A = \exp(F\Delta)$. For small Δ, the first-order approximation of the exponential function suffices, which is

$$A_0 \approx I_7 + \begin{bmatrix} 0_{4\times 4} & \frac{1}{2}Q_0 \\ 0_{3\times 4} & -I_3 n \end{bmatrix} \quad \Delta = \begin{bmatrix} I_4 & \frac{1}{2}Q_0\Delta \\ 0_{3\times 4} & I_3(1 - n\Delta) \end{bmatrix} \tag{11a}$$

Hence, the computed a priori covariance matrix at time t_1 is

$$\begin{aligned} P_1(-) &= A_0 P_0 A_0^T + G \\ &= \begin{bmatrix} (p_{q,0} + \eta_q)I_4 + \frac{1}{4}Q_0 Q_0^T p_{\omega,0}\Delta^2 & \frac{1}{2}Q_0 p_{\omega,0}\Delta(1 - n\Delta) \\ \frac{1}{2}Q_0^T p_{\omega,0}\Delta(1 - n\Delta) & I_3[(1 - n\Delta)^2 p_{\omega,0} + \eta_\omega] \end{bmatrix} \end{aligned} \tag{11b}$$

Neglecting terms containing Δ^2 yields

$$P_1(-) = \begin{bmatrix} I_4 a_0 & Q_0 b_0 \\ Q_0^T b_0 & I_3 c_0 \end{bmatrix} \tag{11c}$$

where $a_0 = (p_{q,0} + \eta_q)$, $b_0 = \frac{1}{2} p_{\omega,0}\Delta$, and $c_0 = [(1 - 2n\Delta)p_{\omega,0} + \eta_\omega]$. Consequently, the Kalman gain at time t_1 is

$$\begin{aligned} K_1 &= P_1(-)H^T[HP_1(-)H^T + R]^{-1} \\ &= \begin{bmatrix} I_4(p_{q,0} + \eta_q)/(p_{q,0} + \eta_q + \xi) \\ \frac{1}{2}Q_0^T p_{\omega,0}\Delta/(p_{q,0} + \eta_q + \xi) \end{bmatrix} \end{aligned} \tag{11d}$$

Define

$$\alpha_1 = a_0/(a_0 + \xi) \tag{11e}$$

$$\beta_1 = b_0/(a_0 + \xi) \tag{11f}$$

then K_1 can be written as

$$K_1 = \begin{bmatrix} I_4 \alpha_1 \\ Q_0^T \beta_1 \end{bmatrix} \tag{11g}$$

We realize that K_1 is, indeed, in the form described in the proposition. Using Eqs. (11) and the fact that $Q_0^T Q_0 = I_3$, it can be shown that

$$\begin{aligned} P_1(+) &= (I_7 - K_1 H)P_1(-)(I_7 - K_1 H)^T + K_1 \cdot R \cdot K_1^T \\ &= \begin{bmatrix} \alpha_1 \xi I_4 & \beta_1 \xi (1 + 2\alpha_1) Q_0 \\ \beta_1 \xi (1 + 2\alpha_1) Q_0^T & (3b_0\beta_1 + c_0) I_3 \end{bmatrix} \end{aligned} \tag{11h}$$

Defining the following constants

$$\gamma_1 = \alpha_1 \xi \tag{11i}$$

$$\chi_1 = \beta_1 \xi (1 + 2\alpha_1) \tag{11j}$$

and noting that $3b_0\beta_1 \propto 3\Delta^2 \to 0$, Eq. (11h) can be written as

[¶]The covariance computation channel in the filter algorithm yields the filter gain. It should be noted that the matrices used in the covariance computation channel are not necessarily the true covariance matrices. In fact, in practice, these matrices are the result of tuning [14].

$$P_1(+) = \begin{bmatrix} I_4\gamma_1 & Q_0\chi_1 \\ Q_0^T\chi_1 & I_3 c_0 \end{bmatrix} \tag{11k}$$

Carrying the computation of the gain one step further, we compute

$$P_2(-) = A_1 P_1(+) A_1^T + G \tag{12a}$$

where

$$A_1 = \begin{bmatrix} I_4 & \frac{1}{2}Q_1\Delta \\ 0_{3\times 4} & I_3(1 - n\Delta) \end{bmatrix} \tag{12b}$$

Using Eqs. (11k) and (12b) in Eq. (12a), noting that $\chi_1\Delta \propto \Delta^2 \to 0$, and therefore neglecting products of $\chi_1\Delta$, one obtains, after some algebraic computation

$$P_2(-) = \begin{bmatrix} I_4(\gamma_1 + \eta_q) & Q_0\chi_1 + \frac{1}{2}Q_1\Delta c_0 \\ Q_0^T\chi_1 + \frac{1}{2}Q_1^T\Delta c_0 & [(1 - 2n\Delta)c_0 + \eta_w]I_3 \end{bmatrix} \tag{12c}$$

Using the last expression in

$$K_2 = P_2(-)H^T[HP_2(-)H^T + R]^{-1} \tag{12d}$$

yields

$$K_2 = \begin{bmatrix} I_4 \frac{\gamma_1+\eta_q}{\gamma_1+\eta_q+\xi} \\ \left[Q_0^T\chi_1 + \frac{1}{2}Q_1^T\Delta c_0\right]\frac{1}{\gamma_1+\eta_q+\xi} \end{bmatrix} \tag{12e}$$

Define

$$\alpha_2 = \frac{\gamma_1 + \eta_q}{\gamma_1 + \eta_q + \xi} \tag{12f}$$

$$\tilde{Q}_2\beta_2 = \left[Q_0^T\chi_1 + \frac{1}{2}Q_1^T\Delta c_0\right]\frac{1}{\gamma_1 + \eta_q + \xi} \tag{12g}$$

Then Eq. (12e) can be written as

$$K_2 = \begin{bmatrix} I_4\alpha_2 \\ \tilde{Q}_2^T\beta_2 \end{bmatrix} \tag{12h}$$

Note that $K_{q,2} = I_4\alpha_2$ is, indeed, a diagonal matrix. Moreover, when $\xi \approx 0$, $\alpha_2 \to 1$, therefore, $K_{q,2} \approx I_4$. Also note that $K_{\omega,2} = \tilde{Q}_2^T\beta_2$ has the form $\upsilon[\,pI_3 + [-\boldsymbol{r}\times] \mid \; -\boldsymbol{r}]$, where υ is chosen such that the norm of $\tilde{\boldsymbol{q}}^T \triangleq [\boldsymbol{r}^T \;\; p]$ is unity. One can now continue the computation of $P_2(+)$, $P_3(-)$, K_3, etc. This will yield the general expression

$$K_k = \begin{bmatrix} I_4\alpha_k \\ \tilde{Q}_k^T\beta_k \end{bmatrix} \tag{12i}$$

The approximations made in deriving the expression for K_k have been verified in numerous simulations. In the next section, in which we compute the angular rate using a simple feedback loop, we will take advantage of this unique form of K_q and K_ω.

III. PSELIKA-Based Rate Extraction Feedback Loop

Following the discussion on the form of the gains K_q and K_ω in the preceding section, we use these forms in the block diagram of Fig. 1. For K_q, we simply use the identity matrix I_4. For K_ω, we need to use $\beta_k\tilde{Q}_k^T = \upsilon_k[\,p_kI_3 + [-\boldsymbol{r}_k\times] \mid \; -\boldsymbol{r}_k]$. Based on our experience, we simply use a constant υ and $Q_k(\boldsymbol{q}_m)$, which we denote by Q_m. Consequently, only two parameters (namely, υ and n) need to be determined by tuning. The resultant block diagram is shown in Fig. 2.

We ran a simulation with $\upsilon = 5500$ 1/s and $n = 0.1$ 1/s, which were obtained by tuning. We chose a baseline angular velocity pattern that was composed of a sequence of different features. It included an oscillatory part, abrupt changes, ramps, and a straight line, all at different levels. Using this angular velocity, we generated

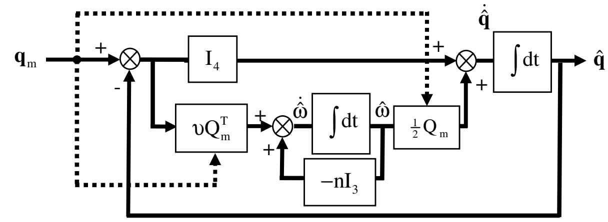

Fig. 2 Block diagram representation of the PSELIKA filter rate estimator.

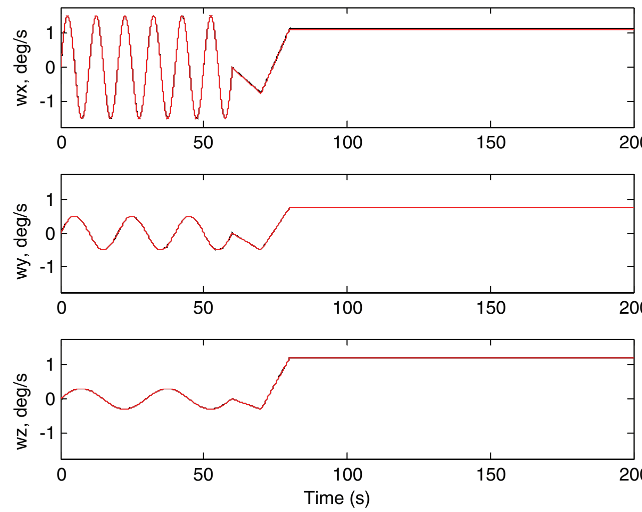

Fig. 3 True (red line) and estimated rate history for the PSELIKA-derived loop.

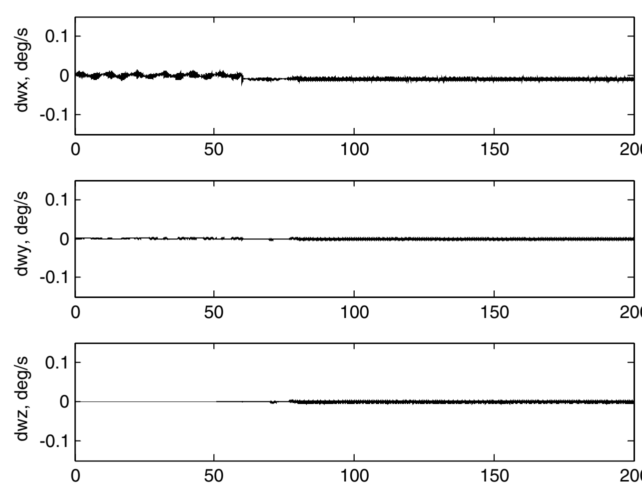

Fig. 4 Rate-estimation error for the PSELIKA-derived loop.

perfect $\boldsymbol{q}_m$. Figure 3 (red line)** presents the nominal baseline angular velocity components, together with their estimates. The components of the rate-estimation error are shown in Fig. 4.

IV. Simple Passive Feedback Systems for Angular Rate Extraction

Borrowing the notion that the angular rate is estimated by a KF in a feedback manner, one can raise the question of whether the rate can be estimated using a simpler feedback loop when the attitude is available almost continuously. The logic behind this concept is as follows. If a feedback loop contains a node that is an input to an integrator, then the variable at this input node is the derivative of the

**This rate will serve as a baseline rate for all the tests that follow.

output of the integrator. If that output is subtracted from the measured quaternion, and the resulting difference is fed forward into the node in a way that drives the difference to zero, or almost zero, then the output of the node is approximately equal to the measured quaternion. Therefore, the variable at the input node is very close to the quaternion time derivative. When the latter is known, then a good estimate of the angular rate can be computed. Before proceeding with the exposition of the feedback control loop schemes, we first show how the angular rate can be computed from the quaternion time derivative.

A. Angular Rate Determination from Quaternion Rate

Using Eq. (1a), we can obtain the following least-squares estimate [15] of $\boldsymbol{\omega}$:

$$\hat{\omega} = 2Q^{\#}\dot{q} \tag{13a}$$

where $Q^{\#}$ is the pseudoinverse of Q, given by

$$Q^{\#} = (Q^T Q)^{-1} Q^T \tag{13b}$$

Using the fact that $Q^T Q = I_3$ and using Eqs. (13a) and (13b), one obtains the following least-squares estimate of the rate vector:

$$\hat{\omega} = 2Q^T\dot{q} \tag{13c}$$

We note that this form corresponds to the form of the K_ω gain of Eqs. (11g) and (12g). The use of Eq. (13c) requires an estimate of $\dot{\boldsymbol{q}}$.

B. Simple Gain Feedback Loop

The simplest control loop for deriving $\dot{\boldsymbol{q}}$ and $\boldsymbol{\omega}$ from the measured quaternion $\boldsymbol{q}_m$ is depicted in Fig. 5. As mentioned earlier, when $\hat{\boldsymbol{q}}$ follows $\boldsymbol{q}_m$, $\dot{\hat{\boldsymbol{q}}}$ follows $\dot{\boldsymbol{q}}$; thus, the estimation of $\boldsymbol{\omega}$ is possible, as indicated in Eq. (13c). When K is a diagonal matrix, the loop is stable for any positive values on the main diagonal of K. A simulation was run of the feedback loop in Fig. 5. The gain matrix K in this simulation was $7 \cdot I_4$. The components of the true and estimated rates

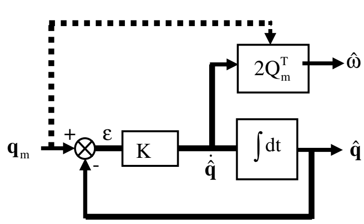

Fig. 5 A simple gain feedback loop for computing a rate estimate.

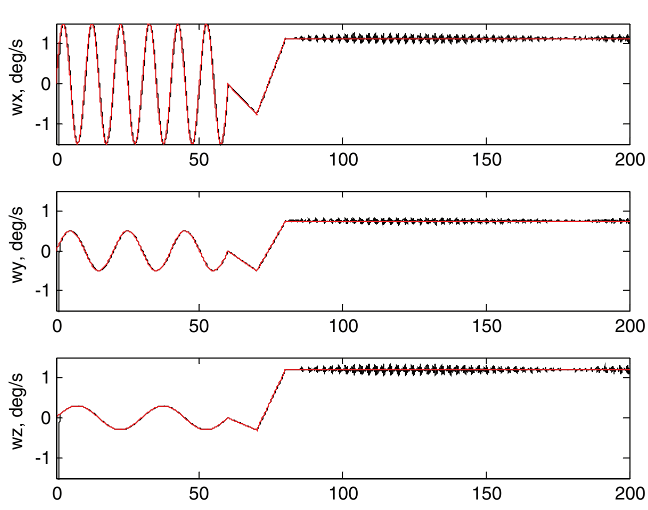

Fig. 6 True (red line) and estimated rate history when using the simple feedback loop.

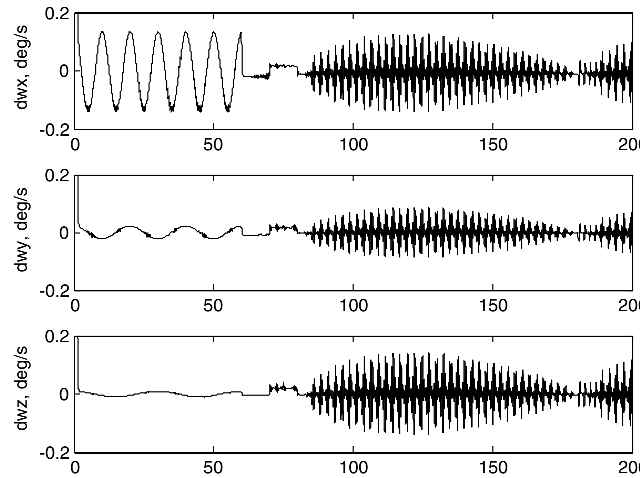

Fig. 7 Rate-estimation error when using the simple feedback loop.

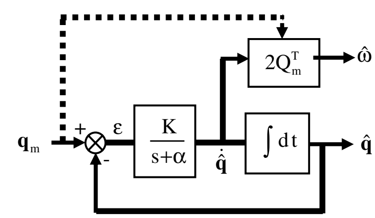

Fig. 8 A stable second-order feedback loop for computing a rate estimate.

are presented in Fig. 6, and the difference between them is shown in Fig. 7.

C. Integral Feedback Loop

The advantage of the previous scheme is its simplicity. Its disadvantage is its limited accuracy. This disadvantage stems from the fact that for very high gains, $\boldsymbol{\varepsilon}$ is a very small signal that contains numerical errors and sensor noise. This noise is then multiplied by a large gain to produce a very noisy $\dot{\hat{\boldsymbol{q}}}$. As a result, the estimated rate is of low fidelity and is also very noisy. On the other hand, for very low gains, $\boldsymbol{\varepsilon}$ is not small; that is, $\hat{\boldsymbol{q}}$ does not follow $\boldsymbol{q}_m$ closely, hence, $\dot{\hat{\boldsymbol{q}}}$ is not close enough to $\dot{\boldsymbol{q}}_m$; therefore, the estimate of the angular velocity is of low quality. If, however, we can isolate $\dot{\hat{\boldsymbol{q}}}$ from $\boldsymbol{\varepsilon}$, then we can keep $\boldsymbol{\varepsilon}$ very low, thereby forcing $\hat{\boldsymbol{q}}$ to follow $\boldsymbol{q}_m$ very closely, and yet maintain the closeness of $\dot{\hat{\boldsymbol{q}}}$ to $\dot{\boldsymbol{q}}_m$. This can be done by replacing K in Fig. 6 with K/s. This, however, will generate a marginally stable loop with poles on the imaginary axis. We stabilize this loop by changing K/s to $K/(s+\alpha)$, which is, basically, a low-pass filter. This loop block diagram is shown in Fig. 8. One can tune K and α to achieve the desirable performance. The components of the true and estimated rates for $K = 10,000$ and $\alpha = 100$ are shown in Fig. 9. The rate-estimation errors are shown in Fig. 10. A comparison between the results of Fig. 10 and the results presented in Fig. 7 indicates that the added low-pass filter reduces the rate-estimation error and eliminates the numerical noise, as well.

V. Rate Estimation with Noisy Quaternion Measurements

In the previous sections, we considered ideal quaternion measurements. It is interesting to examine realistic cases in which the measurements include measurement errors. A typical lateral measurement error of an AST is about 40 arcsec. This translates to about 0.0002 rad. Such white-noise error at a rate of 1 s translates to an equivalent white-noise error of 0.00002 rad when the measurements are taken every 0.01 s, which is the step size of our simulation runs (see Eqs. 8.3–24 in [15]). Using this value as the

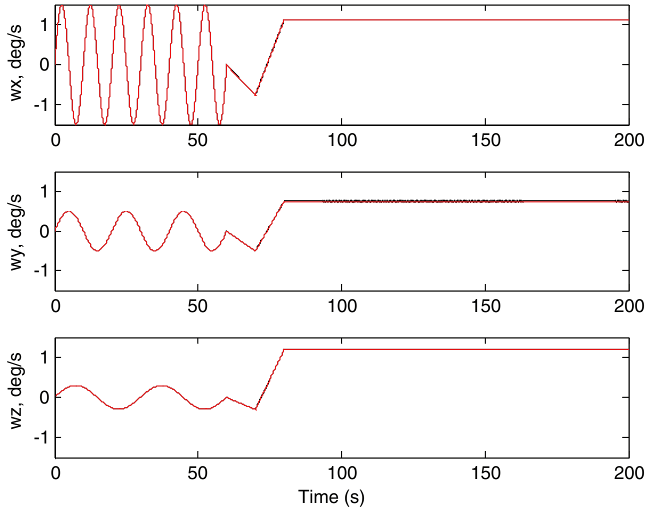

Fig. 9 True (red line) and estimated rate history when using the integrated feedback.

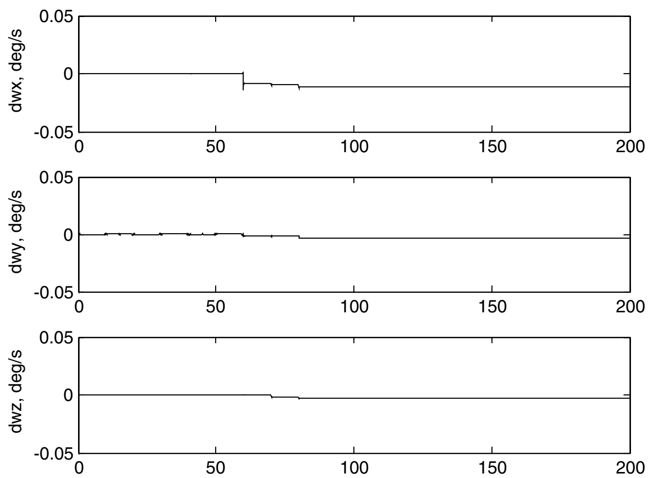

Fig. 10 Rate-estimation error when using the integrated feedback.

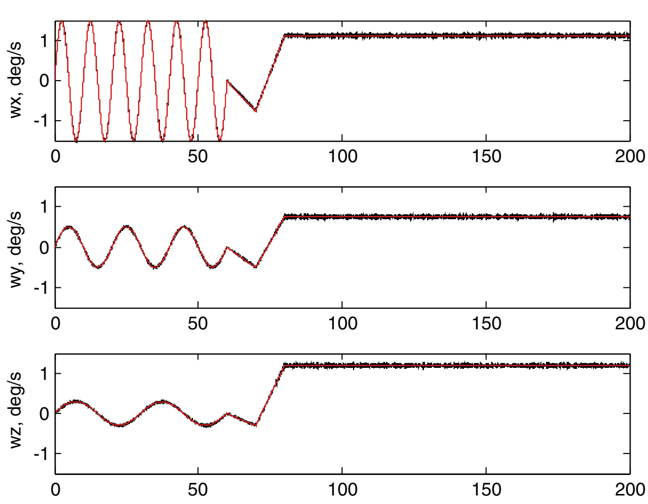

Fig. 11 True (red line) and estimated rate history for the PSELIKA-derived loop.

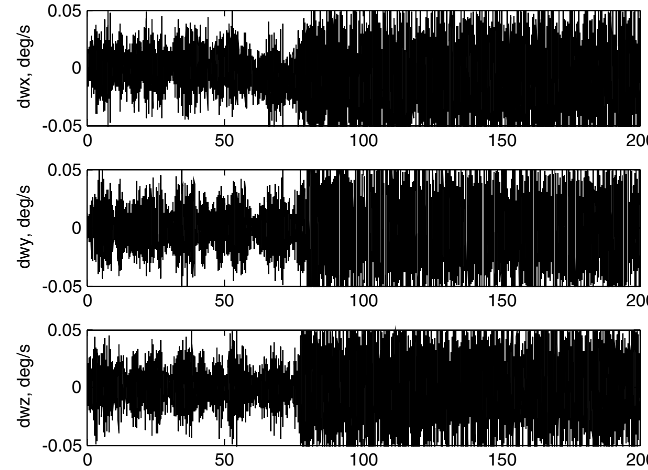

Fig. 12 Rate-estimation error for the PSELIKA-derived loop.

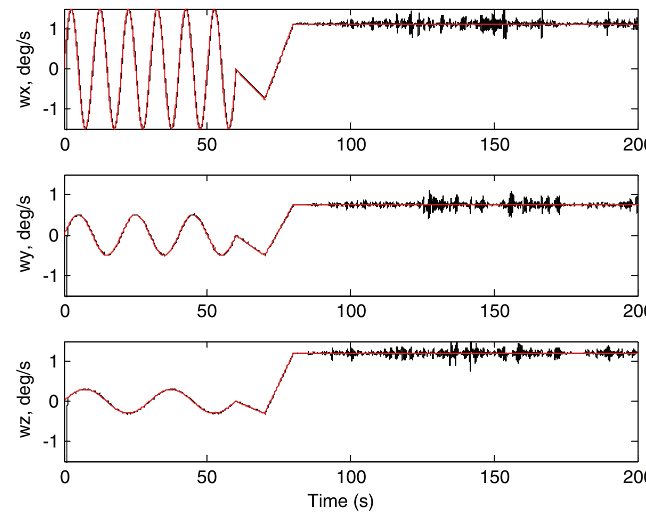

Fig. 13 True (red line) and estimated rate history when using the simple feedback loop.

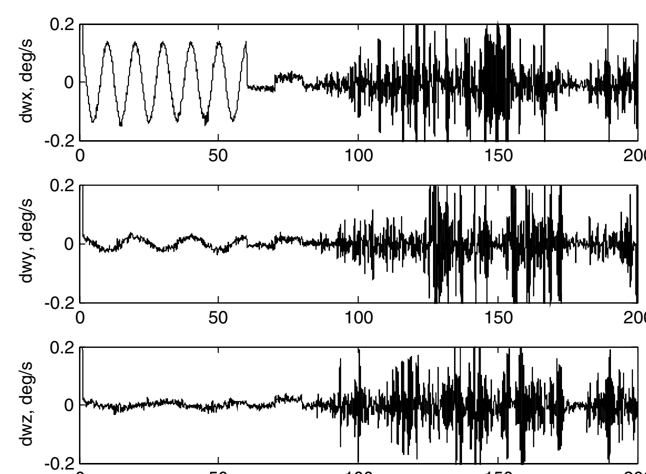

Fig. 14 Rate-estimation error when using the simple feedback loop.

standard deviation (SD) of the measurement noise, we reran the noiseless cases presented in the previous sections. In Fig. 11, we present the true and the estimated rates for the PSELIKA rate-estimation loop (shown in Fig. 2), and in Fig. 12 we present the rate-estimation error. Similarly, Figs. 13 and 14 present the same for the simple gain feedback loop of Fig. 5, and finally, the plots in Figs. 15 and 16 present the results for the stable second-order feedback loop, shown in Fig. 8. The simulations were run with other noise SD levels.

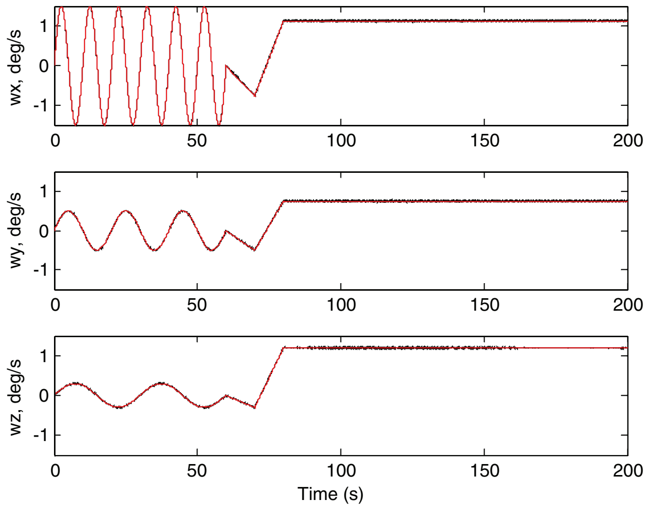

Fig. 15 True (red line) and estimated rate history when using the integrated feedback.

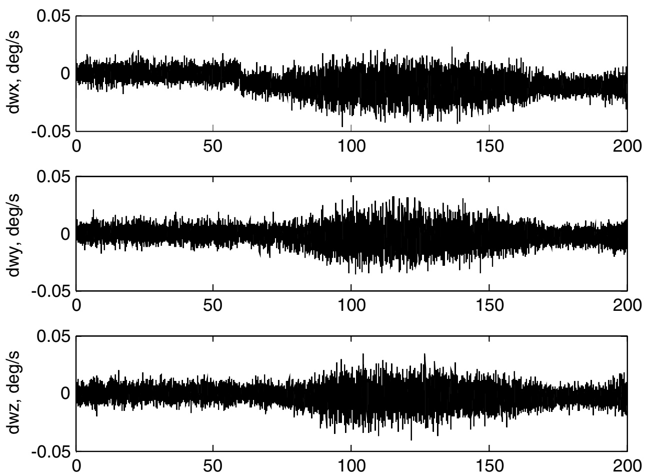

Fig. 16 Rate-estimation error when using the integrated feedback.

Based on all results, it was concluded that adding noise to the measurements induces noise in the estimated rates, but the estimated rate components closely follow the true rate components.

VI. Conclusions

In this work, we investigated the possibility of extracting the angular velocity vector from quaternion measurements without resorting to Kalman filtering. Avoiding Kalman filtering rids us of the cumbersome recursive computation of the covariance matrix. It was found experimentally, and then justified analytically, that when estimating the angular velocity from quaternion measurements using the pseudolinear Kalman filter and a simple dynamics model, the Kalman gain has a peculiar and relatively simple structure. The part of the gain that influences the quaternion estimate is proportional to, and usually very close to, the four-dimensional identity matrix. The part that influences the rate estimate is proportional to the transpose of the Q matrix from the quaternion kinematics equation. Using this quality, a passive feedback loop was designed in which only two scalar parameters had to be tuned to obtain good rate estimates. As mentioned, this feedback loop uses the Q matrix. Therefore, although it is a passive system, it has a time-varying gain and, thus, it is a linear system that is time-varying.

Two other main feedback loops were also introduced that are passive, as well as constant, parameter loops. The loops consist of four simple decoupled loops. The first main feedback loop employs a simple diagonal gain matrix that multiplies the four components of the difference between the estimated and measured quaternion. Each element of the amplified difference is fed into an integrator, the output of which is a component of the estimated quaternion. Therefore, the input to each integrator is the derivative of the estimated quaternion. With these derivatives on hand, the rate estimate is obtained by a known simple linear, time-varying transformation. The second main feedback loop constitutes an improvement of the first one. It contains an added pole that enables a more accurate estimation of the angular rate.

Simulation results indicate that all three feedback systems presented in this work are adequate for deriving the angular rate vector from frequent quaternion measurements for the purpose of attitude control loop damping.

Although we only considered quaternion measurements as input to the rate-estimation feedback loops, vector measurements can also be handled. This is done by applying the method presented in [16], in which a body measured unit vector and its expression in the reference coordinate system are converted into a pseudomeasurement of the quaternion of rotation.[††]

Acknowledgments

A part of this work was supported by a National Research Council–NASA Goddard Space Flight Center Research Fellowship. We would like to thank Mark Koifman of the Philadelphia Flight Control Laboratory of the Faculty of Aerospace Engineering of the Technion—Israel Institute of Technology for performing many of the computer runs.

References

[1] Van Bezooijen, R. W. H., Anderson, K. A., and Ward, D. K., "Performance of the AST-201 Star Tracker for the Microwave Anisotropy Probe," AIAA Guidance, Navigation, and Control Conference, Monterey, CA, AIAA Paper 2002-4582, 2002.

[2] Harman, R. R., and Bar-Itzhack, I. Y., "Angular-Rate Computation Using Attitude Differentiation," Faculty of Aerospace Engineering, Technion–Israel Inst. of Technology, Rept. TAE-881, Haifa, Israel, Dec. 1997.

[3] Bar-Itzhack, I. Y., "Classification of Algorithms for Angular Velocity Estimation," *Journal of Guidance, Control, and Dynamics*, Vol. 24, No. 2, Mar.–Apr. 2001, pp. 214–218.

[4] Oshman, Y., and Markley, F. L., "Sequential Attitude and Attitude-Rate Estimation Using Integrated-Rate Parameters," *Journal of Guidance, Control, and Dynamics*, Vol. 22, No. 3, 1999, pp. 385–394.

[5] Dellus, F., "Estimation of Satellite Angular Velocity Using Sequential Measurements of a Single Inertial Vector," M.S. Thesis, Faculty of Aerospace Engineering, Technion–Israel Inst. of Technology, Haifa, Israel, June 1998 (in Hebrew).

[6] Bucy, R. S., and Joseph, P. D., *Filtering for Stochastic Processes with Applications to Guidance*, Interscience, New York, 1968.

[7] Bierman, G. J., *Factorization Methods for Discrete Sequential Estimation*, Academic Press, New York, 1977.

[8] Harman, R. R., and Bar-Itzhack, I. Y., "Pseudolinear and State-Dependent Riccati Equation Filters for Angular Rate Estimation," *Journal of Guidance, Control, and Dynamics*, Vol. 22, No. 5, Sept.–Oct. 1999, pp. 723–725.

[9] Wertz, J. R. (ed.), *Spacecraft Attitude Dynamics and Control*, Reidel, Dordrecht, Holland, The Netherlands, 1984.

[10] Bryson A. J., "Kalman Filter Divergence and Aircraft Motion Estimators," *Journal of Guidance and Control*, Vol. 1, No. 1, Jan. 1978, pp. 71–79.

[11] Lefferts, E. J., Markley, F. L., and Shuster, M. D., "Kalman Filtering for Spacecraft Attitude Estimation," *Journal of Guidance, Control, and Dynamics*, Vol. 5, Sept.–Oct. 1982, pp. 417–429.

[12] Bar-Itzhack, I. Y., and Oshman, Y., "Attitude Determination from Vector Observations: Quaternion Estimation," *IEEE Transactions on Aerospace and Electronic Systems*, Vol. AES-21, Jan. 1985, pp. 128–136.

[13] Luenberger, D. G., "Observers for Multivariable Systems," *IEEE Transactions on Automatic Control*, Vol. AC-11, No. 2, Apr. 1966, pp. 190–197.

[14] Maybeck, P. S., *Stochastic Models, Estimation and Control*, Vol. 1, Academic Press, New York, 1979, pp. 337–339.

[††]An expanded version of the present Note can be found in [17].

[15] Gelb, A. (ed.), *Applied Optimal Estimation*, MIT Press, Cambridge, MA, 1986, p. 103.
[16] Bar-Itzhack, I. Y., and Cohen, Y., "Geometry Based Euler-Vector and Quaternion Recursive-Estimators," AIAA Guidance, Navigation, and Control Conference, San Francisco, CA, AIAA Paper 2005-6398, 2005.
[17] Bar-Itzhack, I. Y., Harman, R. R., and Thienel, K. J., "A Feedback Approach to Spacecraft Angular Rate Estimation," AIAA Guidance, Navigation, and Control Conference, Keystone, CO, AIAA Paper 2006-6807, 2005.